

Numerical Calculation of a Transient Methane Gas Jet Discharging into Quiescent Atmosphere at Mach One

Felix Chintu NSUNGE^{*}, Eiji TOMITA^{**}
and Yoshisuke HAMAMOTO^{**}

(Received February 18, 1991)

SYNOPSIS

A suddenly started cold methane gas jet issuing from a 1 mm diameter orifice into still air at Mach one has been predicted using the two-equation, high Reynolds number version of k- ϵ turbulence model and SIMPLE algorithm which employs so called primitive variables and a hybrid scheme for treating combined diffusion and convection. Global trends of predicted radial distributions of velocity, temperature, methane concentration in the steady rear part of the transient jet and axial jet tip penetration compare reasonably well with universal profiles representing measurement for the steady jet particularly in the fully developed turbulent core and semi-empirical relation for the transient jet respectively. The prediction scheme has shown reasonably good accuracy especially in prediction of main flow parameters of a transient, high speed compressible gas jet issuing into a dissimilar surrounding gas(binary gas mixture jet).

1. INTRODUCTION

Although experimental and analytical investigation of steady round gas jets has been widely done, available literature indicates that the study of transient gas jets has received relatively less attention. In

* Graduate School of Natural Science and Technology

** Dept. of Mechanical Engineering

the present study, the main flow parameters in a developing transient turbulent methane gas jet has been studied because of its importance in diffusion combustion of stratified fuel-air mixtures in such power plants as furnaces, combustion chambers of internal combustion engines, gas turbine engines and fluid mixing systems in the chemical industry. The flow being turbulent, all the jet flow variables and fluid properties are of course dependent on space and time. Since the jet discharges from the nozzle at Mach higher than 0.3, the general limit for incompressible flow and jet gas is different from the surrounding gas, compressibility was taken into account in the present prediction code by solving complete Navier-Stokes (N-S) equations for compressible flow [1], the governing property transport equation for conservation of chemical species [2], turbulence kinetic energy and its dissipation rate equations [3,4] simultaneously using the SIMPLE algorithm.

The problem solved involves a single shot, methane gas jet issuing from a 1 mm diameter orifice of an automobile fuel injector at an initial sonic velocity, U_0 under atmospheric conditions of the surrounding air. Gas injection continues for 6 ms after which injection is stopped. The present prediction scheme calculates fields of time and space resolved flow variables like the axial and radial velocity, temperature, methane concentration, turbulence energy and its dissipation rate as well as other related flow parameters like density fields of the methane-air mixture, eddy viscosity.

2. PREVIOUS WORK

A brief review of some contemporary experimental and analytical work on fluid jets in general and gas jets discharging into dissimilar surrounding gas in particular is worthy noting at this stage. Unlike many experimental investigations of transient phenomenon including gas jets which usually involve measurement of one or two main variables like velocity or temperature or concentration, one good aspect of successful numerical prediction of more complicated fluid flows especially unsteady compressible flows is that all velocity fields and many related useful variables and parameters like temperature, mass fraction, density, eddy viscosity are solved for simultaneously simply because these variables and properties are so interdependent that no correct solution is possible without solving for all necessary variables and properties.

Many researchers like Abramovich[5], Pai[6], Rajaratnum[7], Schlichting[8], Hinze[9], have done or reported other researcher's

experimental results of main flow parameters in different types of compressible and incompressible steady gas jets. It is mainly this consistent experimental data which are represented by universal profiles like the Gaussian curve[9] or Schlichting's $3/2$ power law[5] for radial distribution of axial velocity or Tollmien's curves[5] for the axial distribution of axial velocity on jet axis or radial variation of radial velocity in incompressible and compressible steady jets up to Mach one.

Experimental work on transient gas jets especially those issuing from small orifices into a dissimilar surrounding gas which is most relevant to the present gas jet calculated in this paper include the transient hydrogen gas jet in air carried out by Hamamoto et al.[10] in which the transient concentration of hydrogen gas was measured using laser interferometry technique, sonic methane gas jet in air carried out by Komoda et al.[11] in which transient concentration of methane gas was measured using chromatography(gas sampling) method, hydrogen gas jet in air done by Tanabe et al.[12] in which transient concentration of hydrogen gas was detected by a special fast response, hot-wire probe employing the property of the binary gas based on heat transfer principle, helium gas jet in air also done by Tanabe[13] in which transient concentration of helium gas was measured by a fast response, hot-wire probe and the transient free laminar carbondioxide gas jet done by Takagi et al.[14] in which transient axial velocity and concentration of carbondioxide jet were measured using LDA and rayleigh light scattering methods for a binary gas mixture at constant pressure and temperature respectively. Transient wall impinging methane gas jets in which transient concentration of methane gas were measured by small probe has been reported by Iida et al.[15] while Witze[16] has measured transient profiles of axial velocity on several locations of the axis of a transient free air jet using hot-film anemometry. The temporal axial jet tip penetration in almost all the above measurements of transient free gas jets was also measured either by high speed Schlieren photography or jet tip arrival time at a known axial location.

Analytical work on steady fluid jet or similar flow include that due to Patankar et al.[17] in which a deflected incompressible combustion exhaust gas jet from a chimney was simulated while numerical prediction of a transient free hydrogen gas jet has been done by Takayama et al.[18] and a transient methane gas jet has been calculated by Komoda et al.[11]. Numerical calculation of fuel gas

injection or gas flow in internal combustion engines has been done by many researchers like Halseman et al.[19] and Gosman et al.[20].

3. GOVERNING EQUATIONS

Assuming axisymmetric fluid flow in the methane-air binary gas mixture which is non-reacting, governing equations are those of conservation of total mass, axial and radial momentum, total energy, turbulent kinetic energy and its dissipation rate as well as that of species mass fraction all of whose respective time-averaged dependent variables, ϕ are $1, u, v, h, k, \epsilon$ and mf . Here, mf is taken to be the mass fraction of methane gas and h is the total enthalpy given by $h = CpT + u^2/2 + v^2/2$, Cp is the specific heat capacity [1,2,20]. The whole set can be represented by the following property transport partial differential equation which represents the complete Navier-Stokes equations plus the k, ϵ and mf equations for fluid flow in cylindrical coordinates.

$$\frac{\partial}{\partial t}(\rho\phi) + \frac{\partial}{\partial x}(\rho u\phi) + \frac{1}{r} \frac{\partial}{\partial r}(r\rho v\phi) = \frac{\partial}{\partial x}(\Gamma_{\phi} \frac{\partial \phi}{\partial x}) + \frac{1}{r} \frac{\partial}{\partial r}(r\Gamma_{\phi} \frac{\partial \phi}{\partial r}) + S_{\phi} \quad (1)$$

where t, ρ, r and x stand for time, mixture density, axial and radial coordinates, Γ_{ϕ}, S_{ϕ} are corresponding effective diffusivity and variable source term whose definitions are given in Table.1.

The $k-\epsilon$ turbulence model constants $C_{\mu}, C_1, C_2, \sigma_k, \sigma_{\epsilon}$ used are [3,4] 0.09, 1.44, 1.92, 1.0, 1.3 respectively while effective Prandtl and Schmidt numbers, σ_h, σ_{mf} are both 0.7. The dynamic eddy viscosity, μ_t is calculated from the following semi empirical relation [3,4];

$$\mu_t = C_{\mu} \rho k^2 / \epsilon \quad (2)$$

3.1 Auxilliary Relations

In addition to the property transport equations (1), auxilliary relations are necessary for closing up the system of equations and connecting the viscosity and density to other variables. Thus the density here is calculated from the ideal gas law, assumed perfect gas mixture laws Joel [21], Reid [22] are used to determine mixture properties as follows. The mass fraction, mf and mole fraction, mof of a given chemical species are related by

$$(mof)_i = (mf)_i / \left\{ \sum_{i=1}^n \left(\frac{mf}{MM} \right)_i \right\} \quad (3)$$

where $i = 1, 2, \dots, n$, n is the total number of component gases in a gas mixture = 2 for a binary gas mixture like the present methane-air mixture which is assumed to be non-reacting and MM is the molecular mass of the component gas.

Table.1 Definitions of Coefficients and Source Terms in Eq.(1)

ϕ	Γ_ϕ	Source Term, S_ϕ
1	0	S'_ρ
u	μ_e	$\frac{\partial}{\partial x}(\mu_e \frac{\partial u}{\partial x}) + \frac{1}{r} \frac{\partial}{\partial r}(r\mu_e \frac{\partial v}{\partial x}) - \frac{\partial p}{\partial x} - \frac{2\partial}{3\partial x}(\mu_e \nabla \cdot \bar{U} + \rho k) + S'_u$
v	μ_e	$\frac{\partial}{\partial x}(\mu_e \frac{\partial u}{\partial r}) + \frac{1}{r} \frac{\partial}{\partial r}(r\mu_e \frac{\partial v}{\partial r}) - 2\mu_e \frac{v}{r^2} - \frac{\partial p}{\partial r} - \frac{2\partial}{3\partial r}(\mu_e \nabla \cdot \bar{U} + \rho k) + S'_v$
h	$\frac{\mu_e}{\sigma_h}$	$\frac{\partial p}{\partial t} + \frac{\partial}{\partial x}\{\mu_e(1 - \frac{1}{\sigma_h})\frac{\partial}{\partial x}(\frac{u^2}{2} + \frac{v^2}{2})\} + \frac{1}{r} \frac{\partial}{\partial r}\{r\mu_e(1 - \frac{1}{\sigma_h})\frac{\partial}{\partial r}(\frac{u^2}{2} + \frac{v^2}{2})\}$ $+ \frac{\partial}{\partial x}\{\mu_e(\frac{1}{\sigma_k} - \frac{1}{\sigma_h})\frac{\partial k}{\partial x}\} + \frac{1}{r} \frac{\partial}{\partial r}\{r\mu_e(\frac{1}{\sigma_k} - \frac{1}{\sigma_h})\frac{\partial k}{\partial r}\} + S'_h$
k	$\frac{\mu_e}{\sigma_k}$	$G - \rho \epsilon + S'_k$
ϵ	$\frac{\mu_e}{\sigma_\epsilon}$	$\frac{\epsilon}{k}(C_1 G - C_2 \rho \epsilon) + \rho \epsilon \nabla \cdot \bar{U} + S'_\epsilon$
mf	$\frac{\mu_e}{\sigma_{mf}}$	0

Notes:

- $\bar{U} = ui + vj$; $\nabla \cdot \bar{U} = \frac{\partial u}{\partial x} + \frac{1}{r} \frac{\partial (rv)}{\partial r}$
 where i, j are unit vectors in x and r directions.
- $G = \mu_e \{ 2((\frac{\partial u}{\partial x})^2 + (\frac{\partial v}{\partial r})^2) + (\frac{\partial u}{\partial r} + \frac{\partial v}{\partial x})^2 + 2(\frac{v}{r})^2 \} - \frac{2}{3} \nabla \cdot \bar{U} (\mu_e \nabla \cdot \bar{U} + \rho k)$

3. s'_ϕ are terms containing correlations involving density fluctuations which have been ignored in the absence of guidance on how they should be modeled while $2/3\rho k$ in momentum source terms may be thought of as additional pressure resulting from turbulence.

Concentration of the entrained air which is needed for evaluating mean physical properties of methane-air gas mixtures required in the present numerical prediction scheme are directly obtained from the following on total species concentration in a gas mixture which means therefore that only the methane gas mass fraction need to be solved for in the main numerical prediction scheme;

$$\sum_{i=1}^n (mf)_i = \sum_{i=1}^n (mof)_i = 1 \quad (4)$$

Mean physical properties, $(GP)_{mm}$ like density, viscosity, specific heat molecular mass of the methane-air mixture are then obtained from following relation;

$$(GP)_{mm} = \sum_{i=1}^n (mof)_i (GP)_i \quad (5)$$

where $(GP)_i$ is the general physical property of a gas component in the gas mixture.

Finally, the molecular dynamic viscosity, μ_1 is evaluated from Sutherland's law[1], molecular species mass diffusion coefficient is evaluated from Gilland's formula[23] while the effective viscosity, μ_e is obtained from the following sum to close the system of equations solved;

$$\mu_e = \mu_t + \mu_1 \quad (6)$$

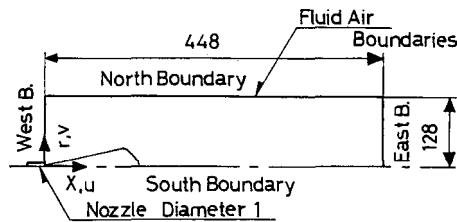


Fig.1 Calculation Domain

3.2 Boundary and initial conditions

As the jet flow is assumed to be axisymmetric, the boundary conditions on the jet axis are $v = 0$ and variable gradients, $\partial/\partial r = 0$. The other three calculation domain boundaries, shown in Fig.1 were considered to be sufficiently far away from the jet and the velocity there was characterized by $u = 0$, $v = 0$ except at the nozzle exit plane. Boundary conditions for temperature on the North and East boundaries were set at room temperature while that on the assumed adiabatic West boundary above the nozzle was taken to be identical to that of the incoming jet gas. It is noted that boundary pressure conditions are satisfied by specified normal velocities at these boundaries[2]. Boundary conditions for mass fraction of methane gas at the east, north and above the injector west boundaries were set at zero.

The boundary conditions for turbulence quantities however require special mention. Friction at the boundaries may be treated by the wall function[3,20] which amounts to assuming one dimensional turbulent

Couette flow near the boundary region in which the universal logarithmic law of wall velocity profile prevails, that diffusion of turbulent kinetic energy is zero and that its dissipation rate is inversely proportional to the distance, y from the boundary all of which may be summarized[19] as follows;

$$C^+ = \ln Ey^+; \quad T^+ = \sigma_h(C^+ + P_f); \quad \frac{\partial k}{\partial y} = 0; \quad \epsilon = C_\mu^{3/4} k^{3/2} / (K_m y) \quad (4)$$

in which C^+ and y^+ are the boundary tangential velocity and normal distance in dimensionless law of wall form, K_m and E are turbulence model and boundary roughness factors whose values are 0.4 and 9.0 respectively for the assumed smooth fluid boundary while T^+ is the dimensionless temperature and P_f is a laminar sub-layer resistance factor. Further detail about origins and implementation of these formulae may be found in the references cited.

For methane gas flow at sonic conditions with room temperature, $T_s = 301$ K and pressure, $P_s = 101.66$ kPa, the initial axial velocity, U_0 estimated from relevant formulae[24] and set uniform across the injector exit plane was 420.8 m/s while the initial exit radial velocity was set to zero. Initial exit temperature, T_0 and density, ρ_0 also set uniform across the nozzle opening and corresponding to above exit sonic conditions were estimated as 261 K and 3.73 kg/m³ respectively while constant initial mass fraction of methane gas, $mf_0 = 1$ was set across the injector exit plane because pure methane was assumed to be injected. The initial turbulence energy, k_0 and its dissipation rate, ϵ_0 were evaluated as follows;

$$k_0 = fu_0^2; \quad \epsilon_0 = C_\mu^{3/4} k_0^{3/2} / l_+; \quad l_+ = SD_0 \quad (5)$$

where f is a factor set between 0.005 and 0.03, l_+ is the length scale[19], S is a length scale factor at inlet between 0 and 1 while D_0 is the initial jet diameter assumed to be identical to that of the nozzle opening. Prior to jet initiation at time, $t = 0$, initial variable, ϕ -field values at all grid points inside the calculation domain were set at actual room conditions, $u = v = k = \epsilon = mf = 0$, $T = T_s$, while those for subsequent timesteps were taken to be equal to the solution fields of the preceding time step.

3.3 Numerical procedure

Using control volume formulation, Eqn.(1) is discretized into a general finite difference equation and the Simple algorithm[2] is used in which pressure fields are first guessed from which tentative velocity u , v fields and subsequently other variable fields are calculated. Their accuracy is checked in the continuity equation before correction, if necessary, is made to the pressure fields. This is repeated in an iteration procedure until the pre-set convergence

criterion like mass efflux in all control volumes or the velocity difference between adjacent iterations within the same timestep at a suitable convergence monitoring point is practically zero and then time is increased until a pre-set total calculation time is covered.

4. RESULTS

4.1 Numerical performance

Coarse computational grids like 21x31, 41x31 stretched at 1.21 and 1.15 in axial and radial directions respectively with the timestep set at 0.2 ms were used with reasonable, but less accurate results before finally using a 51x41 grid stretched respectively at 1.07 and 1.209 with timestep at 0.1 ms for the results presented in this paper. The iteration convergence criteria was set to be attained when the net flow on the whole grid was practically zero or the change in axial velocity, u at a suitable grid node on the jet axis was less than 0.03 m/s between adjacent iterations within the same timestep. With the number of iterations on convergence varying between 20 and 100 per timestep, an average total of about 3600 iterations were executed in each complete run on the ordinary NEC-ACOS2010 Computer. The computer CPU time for one complete run was 340 seconds.

4.2 Predicted results

Only some of the main predicted axial and radial distributions of the main flow variables are presented in this section. Figure 2 shows the predicted axial distributions of time dependent axial velocity, U_m on the jet axis. In the initial and transition regions, the velocities are a bit instable possibly due to combined effect of high initial velocity, appreciably higher pressure, density and methane concentration gradients resulting from the smaller radial thickness of the jet there. When the initial exit velocity is lower and density gradient is low as in the case of subsonic air jet issuing into air, this instability of axial velocity near the injector does not occur in the prediction results[25]. As the jet gas(methane) mixes with the surrounding air, the density gradient decreases with the axial distance so that at downstream locations $x \geq 40$ mm velocities in the steady rear parts of the transient jet stabilise and become steady with time. Steady rear and unsteady front parts of the jet are exhibited at all times during jet gas injection. In both the steady rear and unsteady front parts, the velocity decays with the axial distance, x . However, in the fully developed region the velocity gradient is appreciably higher in the unsteady front region.

Figures 3, 4, 5 and 6 show the respective axial distributions of the predicted instantaneous temperature, mass and mole fractions of methane gas in the methane-air mixture as well as density of the mixture on the jet axis. All these variables exhibit axial profiles which are similar in trend to that of the axial velocity and also have both steady rear and unsteady front parts. The predicted methane gas

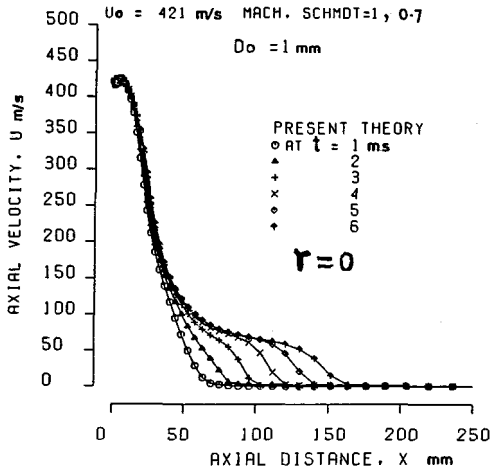


Fig.2 Axial profiles of axial velocity on jet axis

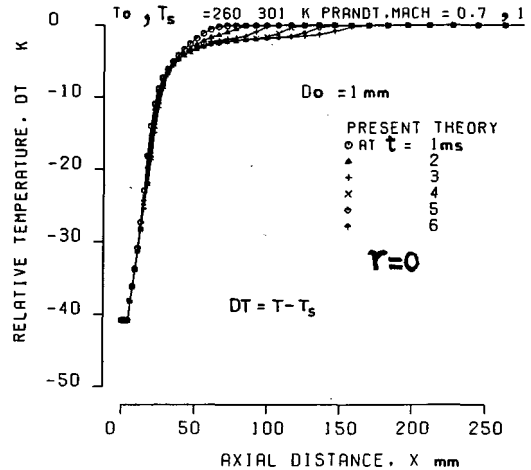


Fig.3 Axial profiles of temperature on jet axis

concentration on the jet axis located in the steady part of the jet compare reasonably well with that obtained by Komoda[11].

Figure 7 shows the predicted instantaneous axial jet tip penetration determined from instantaneous axial distribution of mass or mole fraction of methane gas shown in Fig.4 as locations on the jet axis at which the methane gas concentration reduces to zero. These locations very nearly represent the true jet penetration although it is possible to estimate jet tip penetration from the instantaneous hydrodynamic or thermal tip of the jet using axial distributions of the axial velocity and temperature shown in Figs.2 and 3 respectively[25]. However, particularly when the hydrodynamic jet tip location is used to approximate jet penetration, it may be necessary to introduce appropriate correlation factors which take into account the presence of velocity of the surrounding air being pushed ahead of the jet on the axial velocity profiles shown in Figs.2 because momentum transfer to the surrounding air is much faster than that of energy or chemical species. These correlation factors may be

determined from accurate measurement or prediction of the penetration. Although the present prediction of penetration is higher than that evaluated from semi-empirical formulae for gas and spray penetration [26] by about 10 %, it compares reasonably well with measurement done by Komoda[11].

Figures 8, 9, 10 and 11 show respective instantaneous radial distributions of the predicted temporal axial velocity, radial

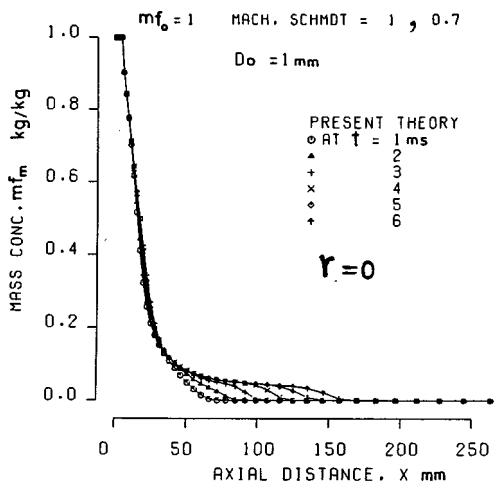


Fig.4 Axial profiles of mass fraction of methane gas

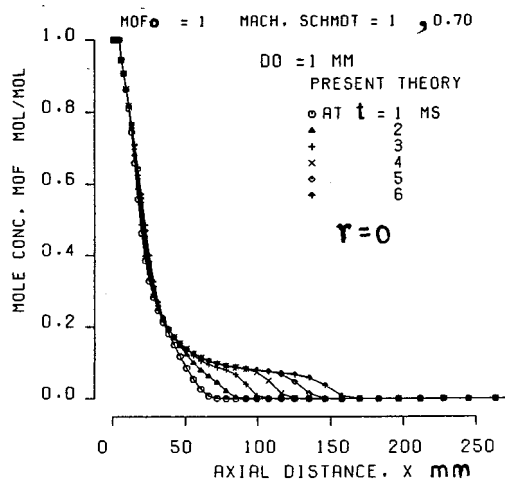


Fig.5 Axial profiles of mole fraction of methane gas

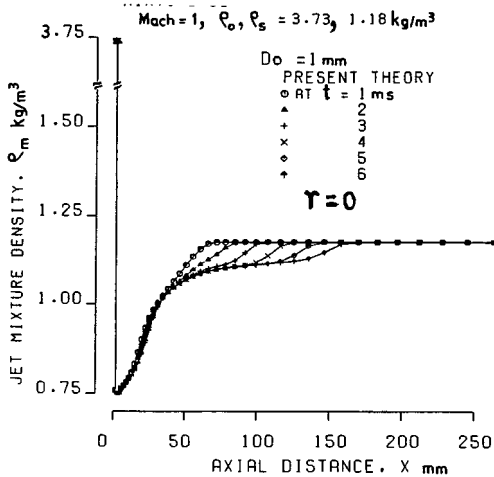


Fig.6 Axial profiles of density of methane-air mixture

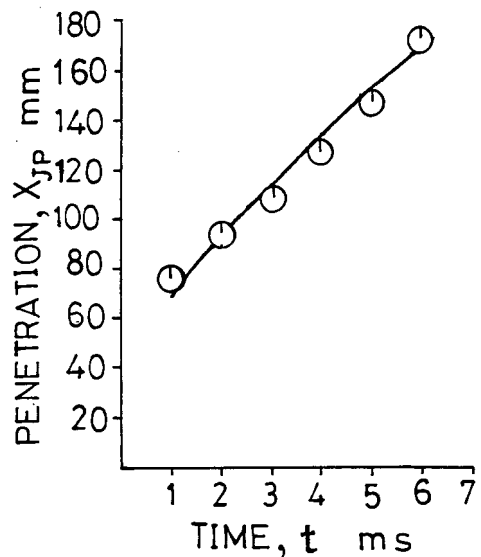


Fig.7 Jet tip penetration

velocity, temperature and mole fraction in the steady rear parts of the transient jet. The abbreviation, ND on axes captions stand for Non-Dimensional. These variables have been normalized by their respective values on the jet axis while radial distances have been normalised by the radius, R_c at which the axial velocity has decayed to one half of that on the jet axis. R_c is determined by interpolation of the predicted axial velocity across the cross section. The distance X_c in the definition of normalized radius for the radial velocity in Fig.9 is the distance along the half- U_m velocity ray which locates the respective cross section from the injector while the value of the

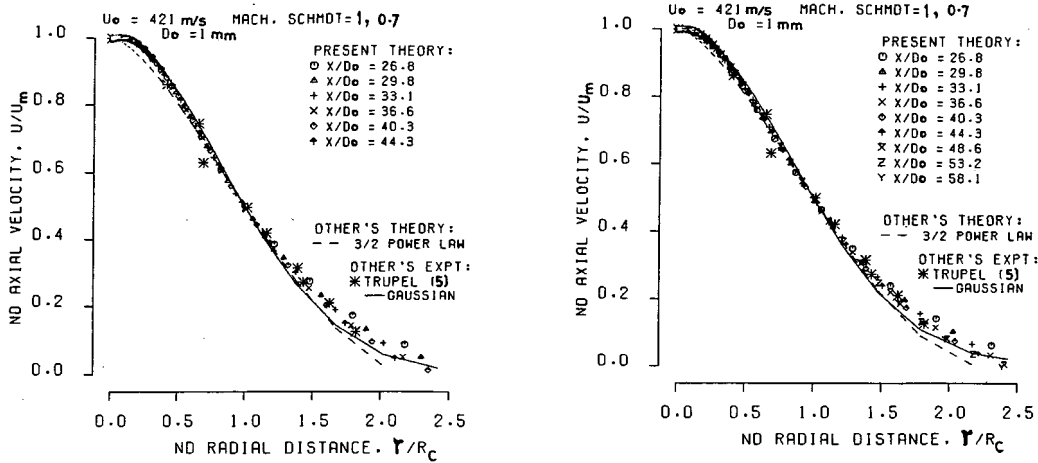


Fig.8 Radial distribution of axial velocity

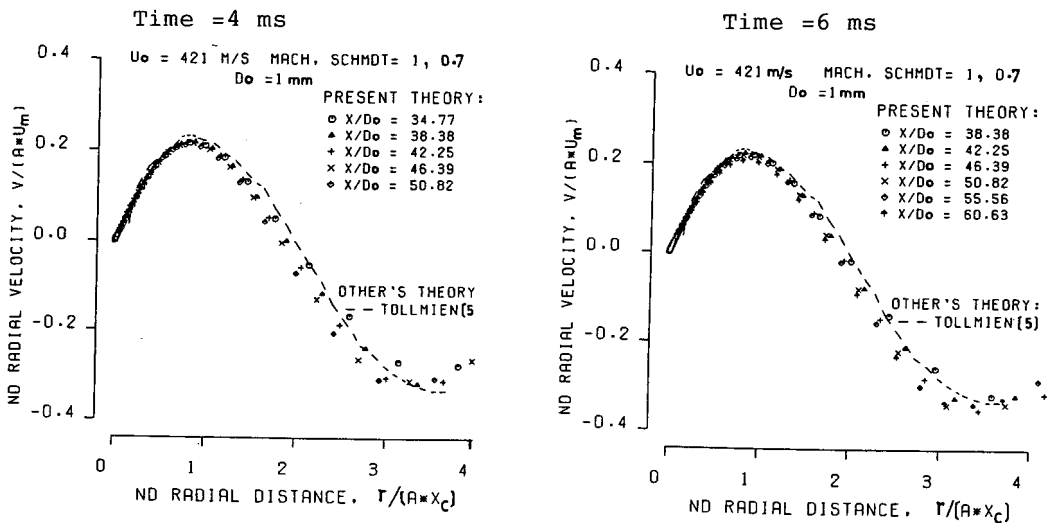


Fig.9 Radial distribution of radial velocity

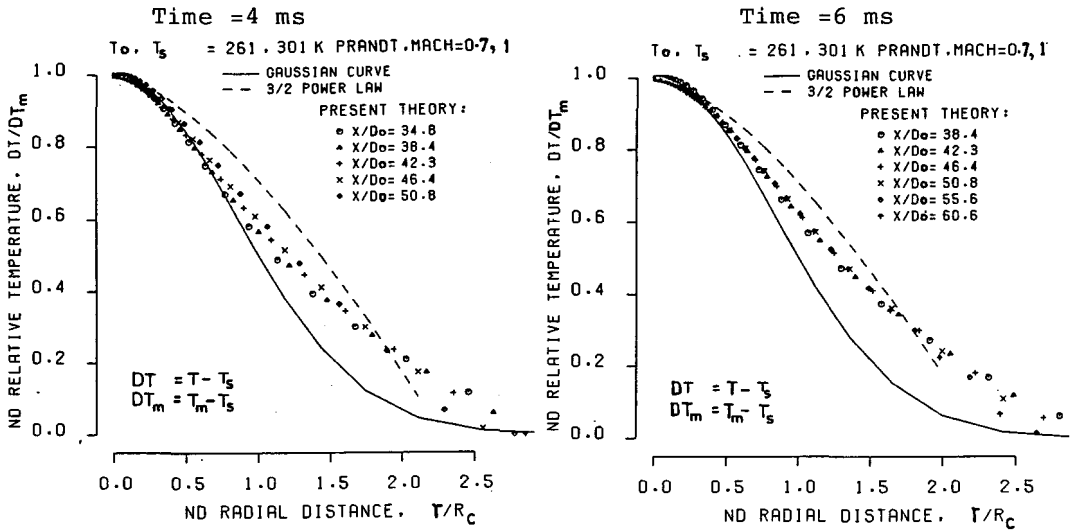


Fig.10 Radial distribution of temperature

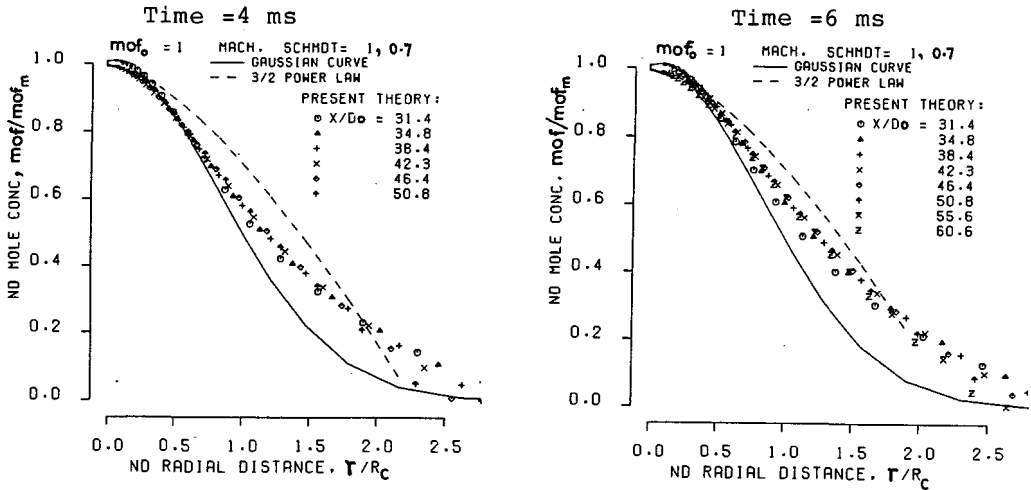


Fig.11 Radial distribution of methane concentration

coefficient, A used is 0.78 [5]. It is worthy noting that radial profiles of axial and radial velocities stabilise to steady states represented by the universal profiles, namely, the Gaussian, 3/2 power laws for axial velocity and Tollmien curves for radial velocity much faster than those of temperature and mass or mole fraction of methane gas. As time progresses, the mole concentration and temperature also spread out radially towards the 3/2 power law for temperature and concentration for the steady jet.

5. CONCLUSIONS

(1) Predicted temporal and spatial distributions of many flow variables seem reasonable particularly in the down stream turbulent core of the jet. As time progresses the jet stabilizes and radial profiles in the steady rear parts of the jet compare reasonably well with universal curves representing the steady jet.

(2) Entrainment may be estimated from predicted axial velocity fields by numerical integration or by using entrainment velocities located on the minima points of the radial distribution of normalized radial velocity.

REFERENCES

1. Anderson, A.A. et al., "Comp. Fluid Mech & Heat Transfer, (1985), McGraw-Hill.
2. Patankar, S.V., "Num. Heat Transfer & Fluid flow", (1980), McGraw-Hill.
3. Launder, B.E. et al., Comp. Methods. Appl. Mech. Eng, Vol. 3, (1974), p.269.
4. Launder, B.E. et al., "Math. Turb. Models", (1972), Academic.
5. Abramovich, G.N., "The Theory of Turbulent Jets", (1963), MIT.
6. Pai, S-I., "Fluid Dynamics of Jets", (1954), Van Nostran.
7. Rajaratnum, N., "Turbulent Jets", (1976), Elsevier.
8. Schlichting, H., "Boundary Layer Theory", 4th Ed., (1960), McGraw-Hill.
9. Hinze, I.O., "Turbulence", 2nd Ed., (1975), McGraw-Hill.
10. Hamamoto, Y. et al., J. Marine Eng. Soc. Japan, (in Japanese), Vol. 25, No. 8, (1990), p. 498.
11. Komoda, T. et al., A Study on Highly Efficient Gas Burning Diesel Engines (in Japanese), Mitsui Zosen Technical Review, No. 121 (1984), p. 46.
12. Tanabe, H. et al., Int. J. Hydrogen Energy, Vol. 7, No. 12 (1982), p. 967.
13. Tanabe, H. et al., 19th FISITA (1982), Paper No. 82026.
14. Takagi, T et al (1988), Int. J. JSME, Series. II, Vol. 31, NO. 1, p. 119.
15. Iida, N. et al., SAE Paper (1990), Paper No. 900479.
16. Witze, P.O., AIAA. J., Vol. 21, No. 2 (1983), p. 308.
17. Patankar, S.V. et al., Trans. of ASME, J. Fluids. Eng, Vol. 99, (1977), p. 758.
18. Takayama, F. et al., Prog. Astr. Aeronaut, Vol. 105, Part. 1, (1986), p. 25.
19. Haselman, L.C. et al., SAE Paper (1978), Paper No. 780318.
20. Gosman, A.D. et al, "Comb. Model. Rec. Engines", (ed., Mattavi, J.N. and Amann, C.A.), (1980), p. 69, Plenum Press.
21. Joel, R., "Basic Eng. Thermodynamics in SI Units", (1971), Longman.

22. Reid, R.C., et al., "The Properties of Gases and Liquids",
4th Ed, (1987), McGraw-Hill
23. Holman, J.P., "Heat Transfer", 4th Ed., (1976), McGraw-Hill.
24. Kumar, K.L., "Engineering Fluid Mechanics", (1980), Eurasia.
25. Nsunge, F.C., et al., Prediction of Transient and Steady Turbulent
Free Subsonic Air Jets, Memoirs of the Faculty of Engineering,
Okayama University, Vol.25, No.2 (1991).
26. Dent, J.C., SAE Trans, Vol.80, (1971), Paper No.710371.